

CHAPTER 3 : RESULTS

3.1 HHV6 Cell Culture

3.1a Light Microscopy

Newly separated cord-blood lymphocytes were single, round and non-granular as seen in Figure 3.1a. After 3 days of growth, uninfected lymphocytes formed clusters (Figure 3.1b). Such lymphocytes were used for infection with HHV6. Centrifugal enhancement (Pietroboni *et al.*, 1989), known to increase the percentage of infection, was routinely used. HHV6 infection led to the lymphocytes becoming single again (Figure 3.2a). Cytopathic effect (CPE) characterised by large “ballooning”, refractile cells, and occasional multinucleated cells (syncytia) were observed 3-5 days post-infection (Figure 3.2b). Clumping of cells was not observed.

3.1b Electron Microscopy of HHV6 Infected HCBMC

Under the transmission electron microscope, presumptive HHV6 capsids of approximately 90-110nm in diameter were observed (Figure 3.3). The cores appeared roughly ring-shaped. Other viral particles appeared to be enveloped particles with a diameter of approximately 150nm, with a thick layer of presumably tegument of 20-40nm around the capsid.

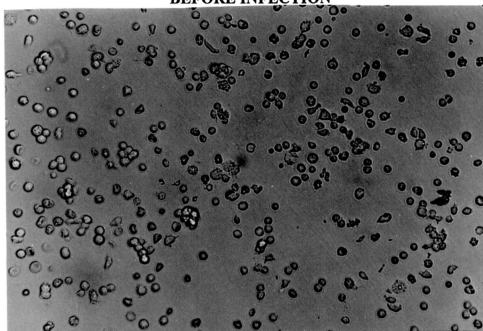
BEFORE INFECTION

Figure 3.1a : Newly separated cord blood lymphocytes are observed to be single, round and non-granular. (Magnification X 200)

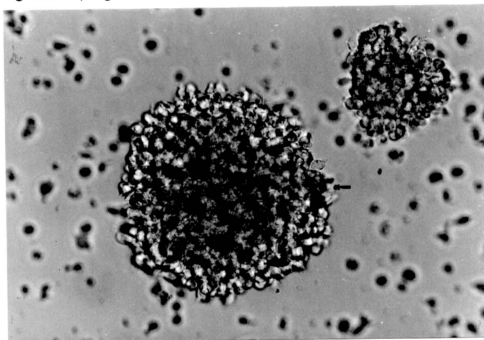


Figure 3.1b : Mature cord blood lymphocytes before infection. Uninfected lymphocytes that form clusters show that the cells are ready for infection. Arrow shows the clumping of cells as observed under the microscope. (Magnification X 200)

AFTER INFECTION

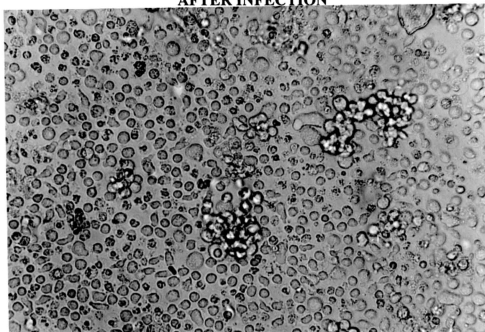


Figure 3.2a : HHV6 infected cord blood lymphocytes at day 0. Once the cells are infected, the cluster becomes single again. (Magnification X 200)

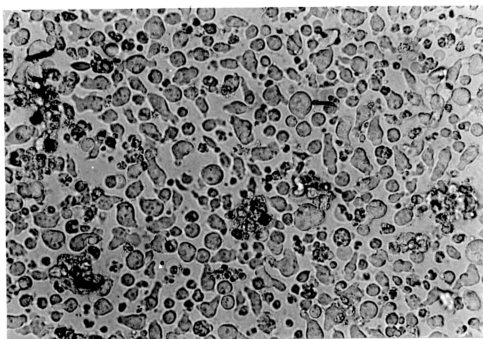


Figure 3.2b : HHV6 infected cord blood lymphocytes at day 3 (before harvesting). The arrow shows cytopathic effects (CPE) characterised by large ballooning, refractile cells as observed under the microscope. (Magnification X 200)

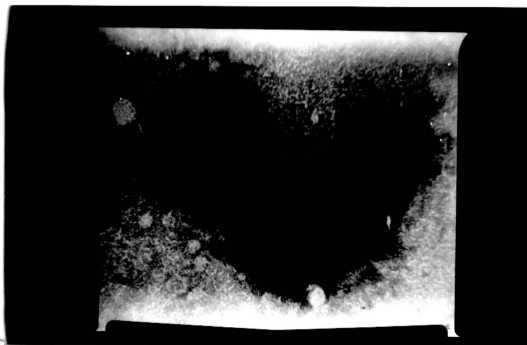


Figure 3.3 : Electron micrograph of extracellular presumptive HHV6 particle. The core is observed as dark structures, roughly ring shaped. The nucleocapsid is coated with a distinct tegument (indicated by the arrow as T). An envelope enclosing the tegument can also be observed. (labelled as E).

┌─┐ Bar = 100 nm

3.2 Detection of HHV6 Antibodies in Age Groups Between 0– 20 years by IFA.

3.2a Serum IgG

For IgG, 20 random sera samples were tested per age group, totalling up to 240 sera samples. The antibody level was highest in the age group 0-1, after which the level gradually decreases. After 2 years of age, antibody levels increased again till it reached a plateau which remained consistent till adulthood. The antibody levels during adulthood were found to fluctuate between 90% to 95% (Table 3.1 and Figure 3.4).

3.2b Serum IgA

IFA was done on sera from 240 subjects aged between 0 to 20 years. Twenty sera were tested in each age group. The dilution used for the serum samples were 1:10. Table 3.2 shows the number of positive and negative sera in each age group.

The presence of IgA-HHV6 was not consistent with age and did not correlate with the levels of IgG. A low prevalence of about 20% is observed in the lower age groups, with the exception of ages between 3 - 4 and 5 - 6 which show 55% positivity. Subsequently, the positivity decreases till the age of 9 and increases again to 85% between the ages of 9 – 10. From ages 10 to 20, a decline in serum IgA can be observed. The group, which has the highest number of positive samples (85%), is the group between 9 - 10 (Table 3.2 and Figure 3.4). A correlation study was carried out based on IgG and IgA results to determine if there was any correlation whatsoever between the two immunoglobulin data. We obtained a correlation co-efficient of 0.5248. Using a Null

hypothesis $H_0=0$, $H_0\neq0$, degree of freedom 10 at 5% significance, a t value 2.23 was tabulated. Hence the Null hypothesis was rejected and we say that the correlation between prevalence of IgG and IgA is significant.

Table 3.2 :IgG Seroprevalence to HHV6B by Age using Immunofluorescence Assay

Age Group (years)	No. of Sera Tested	Seropositivity	
		Number	%
0 – 1	20	16	80
>1 – 2	20	11	55
>2 – 3	20	13	65
>3 – 4	20	14	70
>4 – 5	20	15	75
>5 – 6	20	16	80
>6 – 7	20	17	85
>7 – 8	20	16	80
>8 – 9	20	19	95
>9 – 10	20	18	90
>10 – 15	20	19	95
>16- 20	20	18	90
Total	240		

Table 3.1 : IgA Seroprevalence to HHV6B by Age using Immunofluorescence Assay

Age Group (years)	No. of Sera Tested	Seropositivity	
		Number	%
0 – 1	20	4	20
>1 – 2	20	5	25
>2 – 3	20	5	25
>3 – 4	20	11	55
>4 – 5	20	4	20
>5 – 6	20	11	55
>6 – 7	20	8	40
>7 – 8	20	6	30
>8 – 9	20	7	35
>9 – 10	20	17	85
>10 – 15	20	13	65
>16- 20	20	11	55
Total	240		

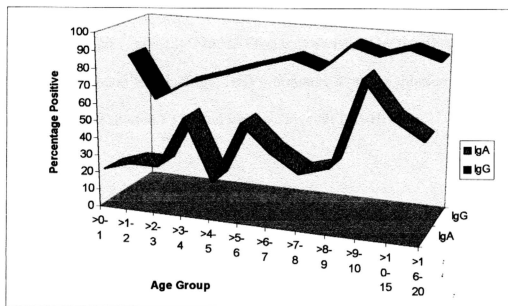


Figure 3.4 : Seropositivity profiles of IgA and IgG HHV6 in different age groups

3.3 Detection of Antibodies against HHV6 Antigens by Immunofluorescence Assay

3.3a Detection of Specific Serum IgG

The presence of IgG to HHV6 antigens assayed by the IFA is shown in Table 3.3. All the 98 infant sera had IgG-HHV6 titratable at serum dilution 1 : 10. All cord blood samples were diluted 1 : 10 and were positive for IgG-HHV6.

3.3b Detection of Specific Serum IgA

Results of IgA response in serum, saliva and cord blood samples are shown in Table 3.4. The 10 cord blood samples that were positive for IgG-HHV6 were negative for IgA-HHV6. Cord blood samples and serum samples were diluted 1 : 10. Of 12 sera obtained from one-month old infants, 6 had IgA-HHV6 while 6 were negative for IgA-HHV6.

Of 20 breast milk samples, 9 were positive. Breast milk was tested without prior dilution, and the conjugate was used at 1:20. None of the 8 saliva samples collected from healthy volunteers showed the presence of IgA-HHV6. Saliva was tested without prior dilution while conjugate was used at 1:20.

Figures 3.5a and 3.5b show negative and positive immunofluorescence in the HHV6 IFA.

Table 3.3 :Presence of IgG-HHV6 in serum and cord blood samples detected by IFA

Serum Samples	No. Tested	No. Positive	% Positive
Infant sera *	98	98	100
Cord blood samples	10	10	100

Sera and cord blood diluted 1 : 10.

* Infant aged between 0 – 1 year old.

Table 3.4 :Presence of IgA-HHV6 in serum, saliva and cord blood samples detected by IFA

Samples	No. Tested	No. positive	% Positive
Cord Blood	10	0	0
Sera from one month old babies	12	6	50
Breast milk	20	9	45
Saliva	8	0	0

Dilution used for cord blood was 1 : 10. Saliva and breast milk used were undiluted.

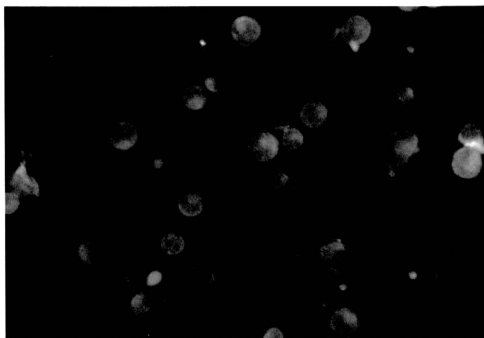


Figure 3.5a : Negative HHV6 immunofluorescence assay. No immunofluorescence is observed in the cells. (Magnification X 200)

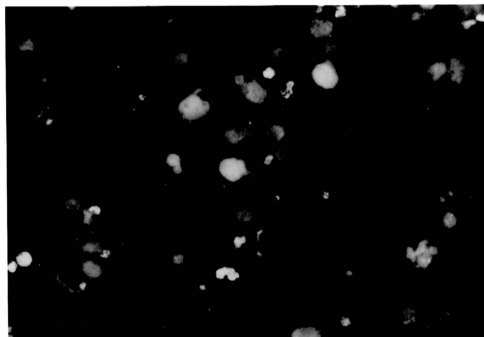


Figure 3.5b : Positive HHV6 immunofluorescence assay. A punctate distribution is observed inside the cells. (Magnification X 200)

3.4 Linear Epitope Mapping of p101 Nucleocapsid Protein of HHV6

The sequence of the 334 amino acids synthesized can be referred to at Figure 2.2, Section 2.8. The method of amino acid sequence selection would be discussed later. The overlapping peptides that were synthesized can be referred to in Appendix 2.

3.4a Epitope Mapping of the HHV6 p101 Carboxyl Terminal Protein

The 46 peptides (14-residue peptides with an overlap of 7 amino acids) were synthesized based on the sequence selected from a hydropathy plot by Hopp and Woods (1981) and synthesized onto non-cleavable pins according to Geysen *et al.* (1984, 1987a). Each peptide was synthesized in duplicates to ensure the repeatability of the resulting ELISA. The peptides were then scanned for reactivity using sera, saliva and breast milk from people who were IFA -positive and IFA-negative in the HHV6 immunofluorescence test.

To facilitate the analysis of the peptide data, a plot was drawn. This is especially useful as human sera usually yield a high background and sometimes no signal could be concluded as significant. This poor signal to background ratio is usually because the serum tested lacks a major population of antibodies directed towards a linear epitope of the immunodominant region. The small peaks observed are believed to be due to recognition of discontinuous epitope segments.

3.4b Conjugate Scanning

Before using the peptides to scan sera samples, a conjugate test was done on the pins as recommended by the manufacturer to ensure that the pins were synthesized properly. As no primary antibody is used during conjugate testing, the readings observed would only be for conjugate binding , thus being very low. Figure 3.6 shows the result of the conjugate test as compared with positive sera.

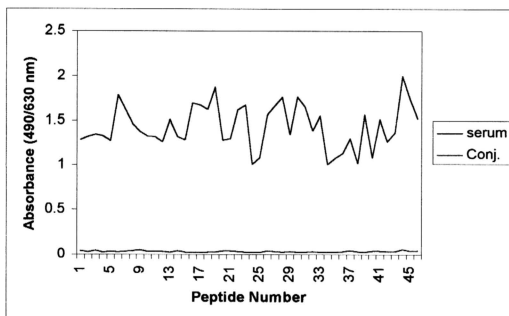


Figure 3.6: Comparison between positive sera and conjugate testing.
sera : average of all positive ELISA readings
conj. : conjugate test readings.

3.4c IgG Epitopes of HHV6 p101 Carboxyl Terminal Protein

3.4c (i) HHV6 IFA-positive serum

Using the modified ELISA, 25 human sera positive for IgG-HHV6 by IFA were scanned against the pins containing overlapping peptides of the 334 amino acids of p101. Profiles of 15 of the 25 sera are depicted in Figure 3.7.

Characteristically, epitopes recognized can either be as isolated peptides or as regions (Naidu, PhD thesis, 1997). HHV6 showed reactivity with peptide regions as well as single isolated peptides and with several adjacent peptides. It is possible for an epitope to be shared by adjacent peptides, only one of which may show maximal reactivity. We consider a peptide to represent a true epitope when at least 3 adjacent peptides showed significant reactivity. However, as man is a highly outbred species, only epitopes which recognized by most, preferably all seropositive individuals are considered to be useful for serological purposes (Middeldorp and Moleon 1988).

Figure 3.8 shows the average positive values of the sera. An average was taken of the 46 peptides for all the positive readings and plotted. A cut-off value of 1.5 was calculated using the mean + standard deviation (SD) formula. (Bernie *et al.*, 1996) Table 3.4 shows the regions recognized. It can be observed that 6 regions showed increased reactivity. Of the 6, only two showed significant activity (peptides 19 and 44-45). It has been mentioned earlier that HHV6 peptides can be either single or appear as regions, peptide 19 is a single peptide whereas peptides 44-45 fall under the region category.

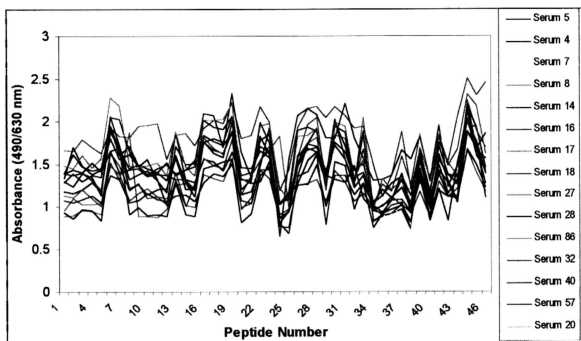


Figure 3.7 : Peptide reactivity profile for 15 HHV6 IFA-positive sera. A similar profile pattern can be observed in all the 15 sera.

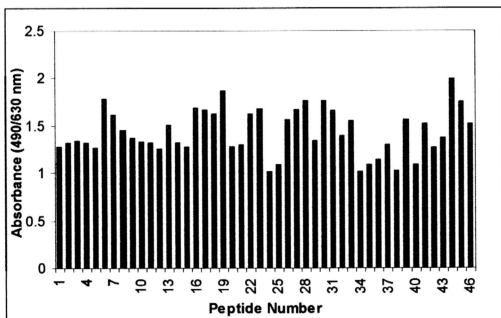


Figure 3.8 : Peptide reactivity profile of HHV6 IFA- positive samples. Graph plotted as the average of the positive ELISA readings.

Table 3.4 :Major regions of HHV6 p101 peptides reactive with IgG in HHV6 IFA- positive sera

Peptide	Sequence	No. Positive	% Positive
6-7	HSREVTDGSGDATETVT ARDS	17	68
16-19	FNVDKEMTQNEQEPLPN LMEAARNAGEEQYVQA GL	21	84
22-23	LAEFTNLISLGEKGIQDI LHN	11	44
26-28	LPTENKLGRESEEEANVE RILEVSDPQNL	12	48
30-31	FKNFKLQNDLDSVQNDL DSVQSPFRLPN	11	44
44-45	IRQDGETDEETVPGVAE SL	24	96

Of these peptides, peptide 44 was consistently recognized by 24 sera tested.

Peptide 19 was strongly recognized by 22 sera.

3.4c (ii) HHV6 IFA-negative serum

When two HHV6 IFA-negative sera were scanned against the same peptides, a totally different profile was observed (Figure 3.9, Table 3.5), with the exception of peptide 31. Figure 3.9 shows a plot of the average ELISA values to the 46 peptides by the two negative sera. It is noted that the peptides that gave high readings with the IFA-positive sera are located close to the peptides that gave high reactivity for IFA-negative sera. The fact that the reactive areas are separated by non-reactive regions supports the suggestion that immunologically important epitopes of HHV6 are probably discontinuous epitopes, assembled by the proximity of various parts of the folded protein. A cut-off of 0.45 was calculated by the method described earlier, thus making peptides 14-15 and 29 significantly reactive.

An interesting observation is that peptides 6-7, 19, 26-28 and 44-45 that were most reactive with the IFA-positive sera, did not show high reactivity with IFA-negative sera. Peptide 31 was picked up by both IFA-positive and IFA-negative sera, indicating that it was not HHV6 specific.

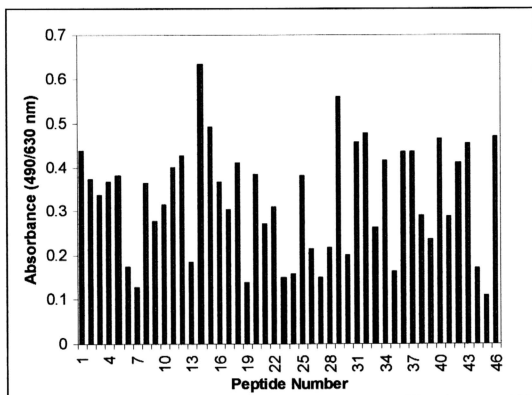


Figure 3.9 : Peptide reactivity profile of HHV6 IFA-negative samples. Graph plotted as the average ELISA reading to the 46 peptides of the two negative sera was taken.

Table 3.5 : Regions of HHV6 p101 peptides reactive with IFA-negative serum samples

Peptide	Sequence	No. Positive	% Positive
14-15	YSGGNAEKKETSGKFNV DKEM	2	100
29	VSDPQNLFKNFKLQ	2	100
31-32	NDLDSVQSPFRLPNADLS RDL	2	100
40	DETLIPTOLMKVET	2	100
43	IEKMVLRIRQDGET	2	100
46	PGVAESLGIAAKDK	2	100

3.4c (iii) Comparison of IgG epitopes identified in HHV6 IFA-positive and negative sera

Figure 3.10 is a net reactivity plot for the HHV6 p101 carboxyl terminal protein for IgG studies. A net ELISA reading for each well was calculated by subtracting the average reading of all negative sera from the average reading of all the positive sera. This net ELISA reading represents any area of the protein where there was a clear differential between the positive and negative. From the net ELISA plot, a cut-off value of 1.4 was calculated using the mean plus standard deviation formula. The peptides that gave the highest reactivity were peptides 6-7, 19, 27 -30 and 44-45 (Figure 3.10). These peptides, highly reactive with the IFA-positive sera and not significant with the IFA-negative sera suggest that it might contain an HHV6- specific epitope.

A frequency profile was then plotted to indicate the number of IFA-HHV6 positive sera giving significant ELISA titers with each of the 46 peptides (Figure 3.11).

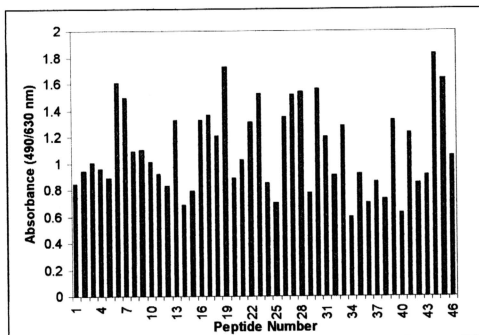


Figure 3.10 : The net ELISA readings for the peptides representing the p101 carboxyl terminal protein. Net ELISA readings for each well was calculated by subtracting the average reading of all negative sera from the average reading of all the positive sera. The peptides that gave the highest reactivity were peptides 6-7, 19 and 44-45.

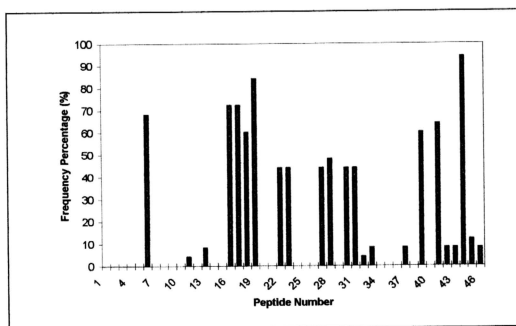


Figure 3.11 : Major epitopes recognized by the 25 IFA-positive infant sera

Eleven peptides bound to different sera with a frequency ranging from 4% (peptide 11) to 96% (peptide 44). Peptide 44 was the immunodominant IgG epitope with all except one serum. Peptide 19 failed to react with 4 sera samples, giving a reactivity percentage of 84% and peptide 6 gave a reactivity of 60% since it did not with 8 sera.

Despite the high level of individual variability, the epitope clusters can be identified that represent areas recognized by multiple individuals. From Figure 3.11, we can see that peptide 6, 19 and 44 show highest reactivities and may be possible antigenic determinants but peptide 44 shows the highest peak for all sera.

A comparison between negative and positive sera is shown in Figure 3.12. From the graph we see that certain regions of the positive and negative sera are mirror images of each other. This is especially clear at peptides 6, 13, 17-19, 27-28, 30, 39, 41, and 44 whereby a peak for the IFA-positive serum was associated with a very low reading in the IFA-negative. Our results suggest that the 3 most probable antigenic determinants as determined by serum IgG are peptides 6, 19 and 44.

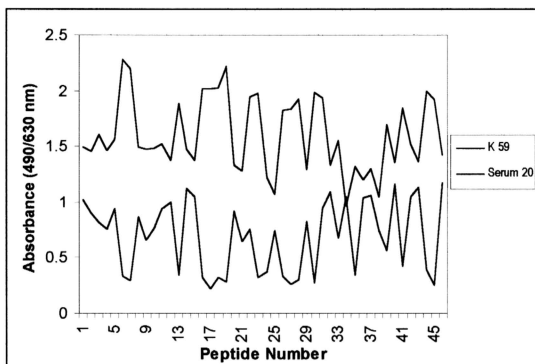


Figure 3.12 : Comparison of HHV6 IFA-negative (serum K59) and IFA-positive (Serum 20) serum profile against peptides of the p101 protein.

3.4c IgG Epitopes of HHV6 p101 Carboxyl Terminal Protein in Breast Milk

3.4d (i) HHV6 IFA-positive breast milk

Twenty breast milk samples were tested in the immunofluorescence assay where 9 were found positive and 11 negative. Six of the 9 IFA-positive breast milk samples and three of the 11 IFA-negative samples were scanned against the pins. A profile of the 6 IFA-positive breast milk is depicted in Figure 3.13.

Figure 3.14 shows the average positive ELISA value of the breast milk samples. An average was obtained for the 46 peptides of the IFA-positive breast milk and the graph plotted. The cut-off value was calculated as 2.2. Table 3.6 shows the regions recognized. It can be observed that 9 regions showed increased reactivities. Of the 9, highest activity was obtained for peptides 2-3, 9, 13, 23, 41 and 43-44. It can be observed that the peptides exist either as single peptides or as regions.

Of all these peptides, all the 6 breast milk tested consistently recognized peptides 2-3, 23, 37, 41 and 44. Peptide 23 and 26 were recognized by 5 samples.

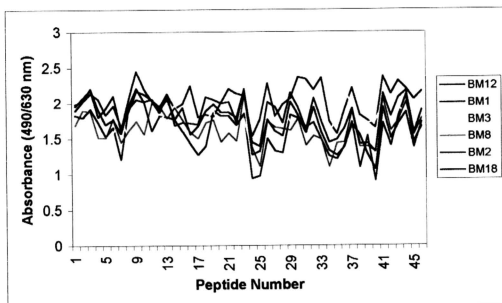


Figure 3.13 : Peptide reactivity profile of 6 HHV6-IFA positive breast milk. A similar profile pattern can be observed in all the 6 breast milk samples. Nine regions showed increased reactivity but the highest activities were obtained for peptides 2-3, 9, 13, 23, 41 and 43-44.

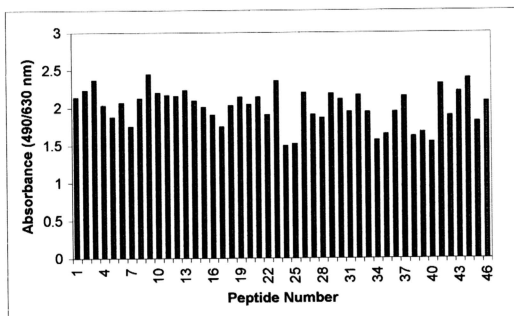


Figure 3.14 : Peptide profile with HHV6 IFA-positive samples. An average ELISA reading was taken of all the 6 breast milk for each of the 46 peptides and the graph plotted.

Table 3.6 : Major regions of HHV6 p101 peptides reactive with IFA-positive breast milk

Peptide	Sequence	No. Positive	% Positive
2-3	RDKDGFRKQKKDLLG SWTKE	6	100
9-13	PVLRKTKHANDIFAGLN KKYARDVSRGGKGNSR DLYSGGNAE	6	100
23	ISLGEKGIQDILHN	5	83
26	LPTENKLGRESEEA	4	66
29-30	VSDPQNLFKNFKLQNDL DSVQ	4	66
32	SPFRLPNADLSRDL	5	83
37	DLALQKVKAGERET	6	100
41	QLMKVETPEEKDDV	4	66
44-45	IRQDGETDEETVPGVAE SLGIAAKDK	5	83

3.4d (ii) HHV6 IFA- negative breast milk

The same peptides were used to screen 3 IFA-negative breast milk and a profile more or less similar to the IFA-positive breast milk profile was observed (Figure 3.15, Table 3.7) with the exception that peptide 13 was not reactive with the IFA-negative samples. This suggests that peptide 13 may contain an HHV6-specific epitope. An interesting observation is that peptides 23, 26, 29, 32 and 37, which were highly reactive with the IFA-positive breast milk were only slightly reactive with the IFA-negative breast milk. For breast milk, peptides 2-3, 9, 41 and 43-44 were picked up by both IFA-positive and IFA-negative samples, indicating that they may not be specific for HHV6. It can be noted that the peptides that gave high readings with the IFA-positive are located close to the peptides that gave high reactivity for IFA-negative sera. The fact that the reactive areas are separated by non-highly reactive regions supports the probability that immunologically important epitopes of HHV6 are discontinuous epitopes, assembled by the various parts of the folded protein.

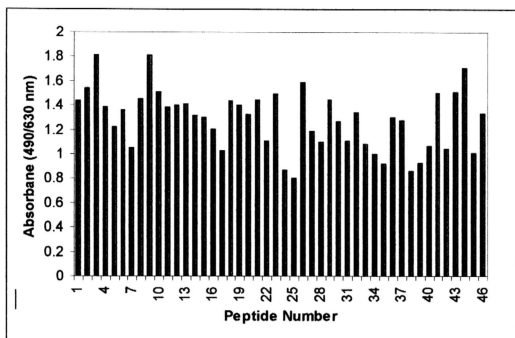


Figure 3.15 : IgA epitopes of HHV6 p101 carboxyl terminal detected in HHV6 IFA-negative breast milk samples.

Table 3.7 : Major regions of HHV6 p101 peptides reactive with IFA-negative breast milk

Peptide	Sequence	No. Positive	% Positive
3	KQKKLDLLGSWTKE	3	100
9	PVLRKTKHANDIFA	3	100
26	LPTENKLGRESEEA	2	67
36-37	GNGEREIDLALQKVKAG ERET	3	100
41	QLMKVETPEEKDDV	3	100
43-44	IEKMVLRIRQDGETDEE TVPG	3	100

3.4d (iii) Comparison of IgA epitopes in HHV6 IFA-positive and negative breast milk

When analyzing and comparing the reactivity of the IFA-positive and IFA-negative breast milk, once again net ELISA readings were plotted. This was calculated by subtracting the average reading of the negative sera from the average reading of the positive sera. This net ELISA reading represents any area of the protein where there was a clear differential between the positive and negative. The cut-off value was calculated as 0.8 and peptides that gave the highest reactivity were peptides 13, 23, 30-33, 37 and 41 (Figure 3.16). These peptides, highly reactive with the IFA-positive sera but not with the IFA-negative sera may contain HHV6-specific epitope.

A frequency profile was then plotted to indicate the number of IFA-HHV6 positive sera giving significant ELISA titers with each of the 46 peptides (Figure 3.17).

Thirteen peptides bound to different breast milk samples with a frequency ranging from 14% (peptides 6 and 18) to 100% (peptide 2,13 and 37). Peptides 2, 13 and 37 were shown to be highly reactive with all samples, recognizing all IFA-positive samples. Peptides 23 and 26 gave a reactivity percentage of 76%.

A comparison profile between IFA-negative and IFA-positive breast milk is depicted in Figure 3.18. It is observed that although the profiles are similar, the negative breast milk gave lower readings compared to the IFA-positive breast milk samples.

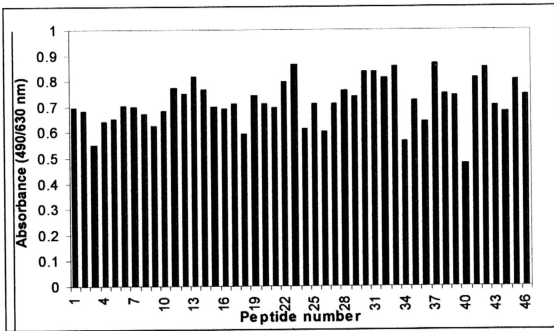


Figure 3.16 : The net ELISA readings for peptides representing the p101 carboxyl terminal protein. Net ELISA reading for each well was calculated by subtracting the average reading of the negative breast milk from the average reading of the positive breast milk. The peptides that gave the highest reactivity were peptides 13, 23, 30-33, 37 and 41.

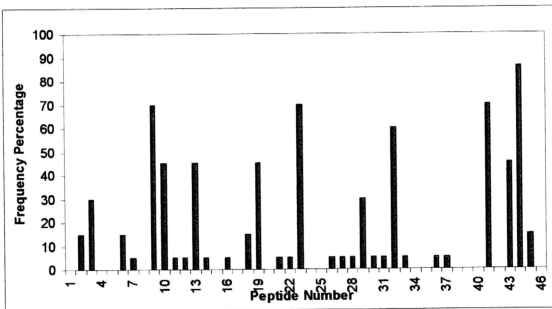


Figure 3.17 : Major epitopes recognized by ELISA in 6 HHV6 IFA- positive breast milk.

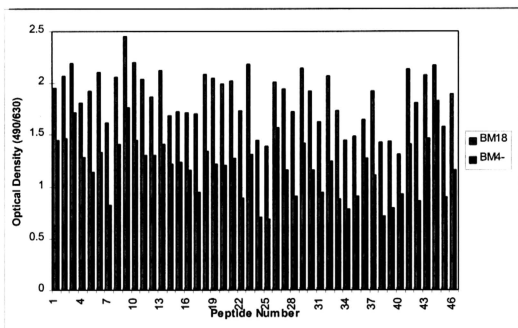


Figure 3.18 : Epitope profile comparison between HHV6 IFA-positive (BM18) and negative breast milk (BM 4-) sample.

3.4e Salivary IgA to Epitopes of HHV6 at the p101 Carboxyl Terminal Protein

Eight salivary samples were tested by IFA on HHV6 infected cells and all the samples tested were negative for IgA. However, when 3 randomly selected saliva of the 8 samples were subjected to peptide-ELISA, all 3 were found to bind to several regions (Table 3.8). The peptides bound were peptide 2, 9, 21, 30 and 44. A profile of the 3 salivary samples is depicted in Figure 3.19. The average ELISA readings for the 46 peptides obtained for the 3 saliva samples are depicted in Figure 3.20. The epitopes were then scored to identify the most reactive epitopes (Figure 3.21).

The binding of saliva to peptides ranged from a frequency of 33% to 100% (peptide 44). Peptide 44 was selected as the most reactive peptide, as it reacted with all 3 saliva samples. Peptides 2, 9, 21 and 30 gave a reactivity percentage of 76%.

Table 3.8 : IgA in Saliva to Linear Epitopes of HHV6 p101 Carboxyl Terminal Protein in Normal Saliva.

Peptide	Sequence	No. Positive (n = 3)
2	RDKDGFRKQKKKLDL	2
9	PVLRKTKHANDIFA	2
21	GQRVNKILAEFTNL	2
30	FKNFKLQNDLDSVQ	2
44	IRQDGETDEETVPG	3

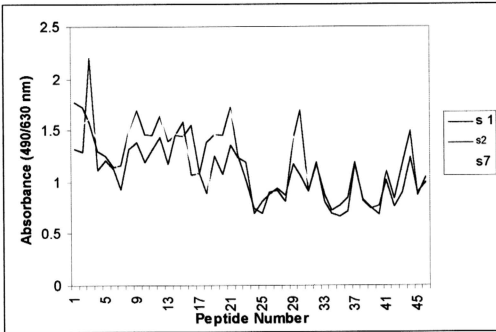


Figure 3.19 : Profiles of salivary IgA to the 46 peptides of HHV6 p101 nucleocapsid protein.

s 1 - saliva 1

s 2 - saliva 2

s 3 - saliva 3

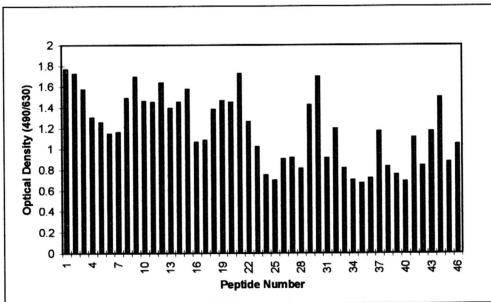


Figure 3.20 : Average salivary IgA to peptides of HHV6 p101 nucleocapsid protein .

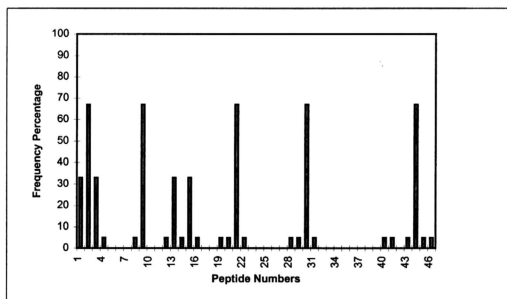


Figure 3.21 : Peptides of p101 nucleocapsid protein recognized by salivary IgA

3.4f Cord Blood IgG to Epitopes of HHV6 p101 Carboxyl Terminal Protein

One cord blood sample was tested for IgG against the peptides and the profile obtained was similar to that from the IFA-positive serum. Figure 3.22 compares the profiles obtained for cord blood and positive serum (serum 40). It is noted that although the pattern is similar, the peaks of the positive serum are higher than those from the cord blood. This could well be due to the higher levels of IgG in serum 40 compared to the cord blood, as cord blood IgG is predominantly maternal IgG.

3.5 Comparison Between Serum-IgG, Salivary-IgG and Breast Milk-IgA to Peptides of HHV6 p101 Carboxyl Terminal Protein

3.5a Serum and Breast Milk

Figure 3.23 shows the profiles of a positive serum and positive breast milk sample, peptide 44 appears as the most reactive region. The regions that showed reactivity with serum but not with breast milk are peptides 6 and 19; additionally the reactivity of the peptides was not high when compared with peptide 44. Conversely, peptides 9, 23 and 41 which were immunoreactive with breast milk did not react significantly with sera samples.

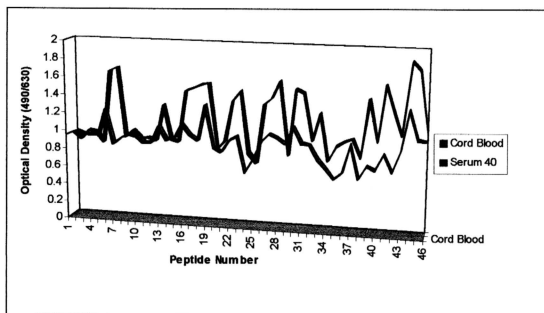


Figure 3.22 : Cord blood and serum IgG to peptides of HHV6 p101 nucleocapsid protein.

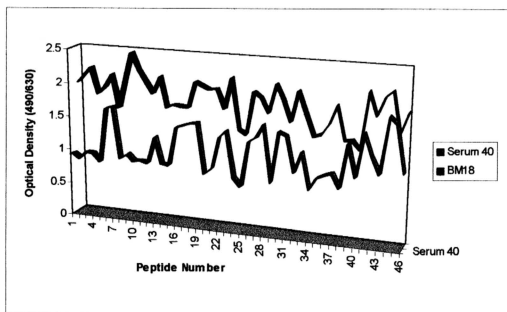


Figure 3.23 : Epitope profile comparison between IgA breast milk (BM18) and IgG serum (Serum 40) to HHV6 p101 carboxyl terminal peptides.

3.6 Hydropathy Plots, Surface Accessibility and Secondary Structure

3.6a Hydropathy Plot

Hydropathy plot was done on the p101 protein of HHV6. Figure 3.26 shows the hydropathy plot, according to the Hopp and Woods method (Hopp and Woods, 1983). The p101 protein contains 858 amino acids. The region selected for the peptide synthesis is from amino acid 534 to 858 from the carboxyl terminus. Figure 3.25 shows the hydropathy plot for the selected region of 334 amino acids.

Based upon studies done on myoglobin and other proteins, antigenic determinants are consistently located at the point of maximum hydrophilicity, the highest points on the hydropathy profiles plotted. However, not all high points were associated with antigenic determinants and not all antigenic determinants can be associated with high points (Hopp and Woods, 1981).

From the 334 that we selected, the plot gave highest hydrophilicity for residues 6-19, 27-32, 39-47, 75-89, 96-103, 108-115, 181-192, 225-234, 246-254, 260-272, 288-295 and 303-313. In the case of our study with serum, 4 of the 6 peptides, which were found reactive, came from the hydrophilic regions (Table 3.9). The peptides, which were reactive and hydrophilic, were peptides 6-7, 16-19, 26-28 and 44-45. As for breast milk, 7 out of 9 peptides deemed reactive fell under the hydrophilic region (Table 3.10). The immunogenic peptide 13, found significant for breast milk fell within the hydrophilic region.

3.6b. Surface Accessibility

Surface accessibility is another characteristic suggested to predict antigenic determinants (Figure 3.26). As accessible regions are regions on the surface of the protein, it would contribute towards the binding between antigens and antibodies. As accessible regions protrude at the surface, the probability of it being recognized by antibodies is higher. In the case of our study in serum, 4 of the 6 peptides, which were found reactive, fell within an accessible region (Table 3.10). The peptides that were reactive and hydrophilic were peptides 6-7, 26-28 and 44-45. An interesting observation was that the region of peptides 16-19, which was categorized as a hydrophilic and antigenic region, did not fall under the accessible category.

As for breast milk, 7 out of 9 peptides found reactive fell under the accessible region (Table 3.12). Peptide 13 which showed higher reactivity in IFA-positive breast milk compared to IFA-negative milk and thus having a possibility of being immunogenic fell within an accessible region. Numerical values for surface accessibility are shown in Appendix 5.

3.6c Secondary Structure

Secondary structure predictions were done according to a method from the DSC programme by Protsacle. (<http://expasy.hcuge.ch/cgi-bin/protscale.pl>) All the recognized peptides, be they IgA-recognized or IgG-recognized have only helices and coils as secondary structures. Residues 57-98 were recognized by breast milk IgA and the region is made up of a coil-helix-coil structure. For IgG analysis, peptides 6-7 has a helix-coil-

helix structure, peptides 16-19 (residue 106-140) a coil-helix-coil-helix structure and peptides 44-45 (residue 302-329) a coil-helix-coil structure.

Figure 3.27 shows the secondary structure prediction of the 334 amino acids residues. The secondary structure predictions for the major peptides for IgA analysis (breast milk and saliva) and serum IgG analysis are shown in Table 3.13 and 3.14. Numerical values of secondary structure calculations are shown in Appendix 6. The three probes found in the secondary structure prediction are E being sheet, C being coils and H being helices. The probe with the highest numerical value becomes the secondary structure of choice.

In addition to the 3 parameters used, we also added mobility (Figure 3.28) and conformational parameter for coil structure (Figure 3.29). Hydropathy plots for both parameters were obtained from Protscale (<http://expasy.hcuge.ch/cgi-bin/protscale.pl>). It has been documented that mobile segments are more likely to be on the surface and therefore more likely to be exposed (Tainer *et al.*, 1984., Westhoff *et al.*, 1984). The mobility hydropathy plot was superimposed on the hydrophilicity as well as the surface accessibility plots. The corresponding IgG peptides were peptides 22-23, 30-31 and 44-45 (Table 3.15). Seven of the nine IgA peptides corresponded to mobility (Table 3.16). However peptide 13 which was highly reactive with IFA-positive breast milk did not fall within the mobile region. To confirm whether IgA could be considered as an antigenic site, tests need to be carried out on more subjects. However, as the prediction of antigenic sites are based on more than one particular method, based on this study, we can accept the data that peptide 13 is a potential antigenic site as it fulfilled the criteria for

hydrophilicity, surface accessibility, secondary structure and coil structure. Numerical value for mobility is shown in Appendix 7.

The analysis on coil structure parameter was done to further confirm the secondary structure prediction profile. However, the predicted coil structure corresponding to their respective peptides is not tabulated in a table. Numerical values for coil structure is in Appendix 8. Coil structures are found at residue numbers 40-49, 80-97, 164-171, 214-249 and 308-321. Coil structures with the highest numerical value are at residues 308-321, which correspond to peptides 44-45. Peptide 13, found reactive in the IgA analysis corresponded to residues 80-97.

Table 3.9 :Hydrophilicity Plot: Predicted Antigenic Regions of HHV6 p101 Carboxyl Terminal Protein and their Corresponding Hydrophilic Amino Acid Residues and IgG Reactivity.

Reactive peptides from IgG epitope analysis	Corresponding amino acid residues	Corresponding hydrophilic amino acid residues from hydropathy plot
6-7	36-56	39-47
16-19	106-140	108-115
22-23	148-168	-
26-28	176-203	181-192
30-31	204-224	-
44-45	302-329	303-313

* Data obtained based on Figure 3.10

Table 3.10 :Hydrophilicity Plot: Predicted Antigenic Regions of HHV6 p101 Carboxyl Terminal Protein and their Corresponding Hydrophilic Amino Acid Residues and IgA Reactivity.

Reactive peptides from IgA peptide analysis	Corresponding amino acid residues	Corresponding hydrophilic amino acid residues from hydropathy plot
2-3	8-28	6-19
9-13	57-98	75-89
23	155-168	-
26	176-199	181-192
29-30	197-317	-
32	219-231	225-231
37	253-266	260-268
41	281-294	288-295
44-45	302-329	303-313

* Data obtained based on Figure 3.16

Table 3.11 :Accessibility Plot: Predicted Antigenic Regions of HHV6 p101 Carboxyl Terminal Protein and their Corresponding Accessible Amino Acid Residues and IgG Reactivity.

Reactive peptides from IgG epitope analysis	Corresponding amino acid residues	Corresponding accessible amino acid residues from accessibility plot
6-7	36-56	40-49
16-19	106-140	-
22-23	148-168	-
26-28	176-203	172-185
30-31	204-224	-
44-45	302-329	325-334

* Data obtained based on Figure 3.10

Table 3.12 :Accessibility plot: Predicted Antigenic Regions of HHV6 p101 Carboxyl Terminal Protein and their Corresponding Accessible Amino Acid Residues and IgA Reactivity.

Reactive Peptides from IgA epitope analysis	Corresponding amino acid residues	Corresponding accessible amino acid residues from accessibility plot
2-3	8-28	25-33
9-13	57-98	74-107
23	155-168	-
26	176-199	172-185
29-30	197-317	-
32	219-231	228-241
37	253-266	257-271
41	281-294	288-293
44-45	302-329	325-334

* Data obtained based on Figure 3.16

Table 3.13 :Reactive Peptides (Serum IgG) which Correspond to Predicted Secondary Structures for Antigenic Regions of HHV6 p101 Carboxyl Terminal Protein.

Reactive Peptides (serum IgG)	Corresponding amino acid residues	Secondary structure predictions
6-7	36-56	helix-coil-helix
16-19	106-140	coil-helix-coil-helix
22-23	148-168	helix-coil-helix
26-28	176-203	helix-coil-helix
30-31	204-224	helix-coil-helix
44-45	302-329	coil-helix-coil

* Data obtained based on Figure 3.10

Table 3.14 :Reactive Peptides (Serum IgA) which Correspond to Predicted Secondary Structures for Antigenic Regions of HHV6 p101 Carboxyl Terminal Protein.

Reactive peptides (serum IgA)	Corresponding amino acid residues	Secondary structure predictions
2-3	8-28	coil-helix-coil-helix
9-13	57-98	coil-helix-coil
23	155-168	helix-coil-helix
26	176-199	coil-helix-coil
29-30	197-317	coil-helix
32	219-231	helix-coil
37	253-266	helix-coil
41	281-294	coil-helix-coil
44-45	302-329	helix-coil-helix

* Data obtained based on Figure 3.16

Table 3.15 :Mobility Plot: Predicted Antigenic Regions of HHV6 p101 Carboxyl Terminal Protein and their Corresponding Mobile Amino Acid Residues and IgG Reactivity.

Reactive peptides from IgG epitope analysis	Corresponding amino acid residues	Corresponding accessible amino acid residues from mobility plot
6-7	36-56	-
16-19	106-140	-
22-23	148-168	147-166
26-28	176-203	-
30-31	204-224	216-224
44-45	302-329	315-328

* Data obtained based on Figure 3.10

Table 3.16 : Mobility plot: Predicted Antigenic Regions of HHV6 p101 Carboxyl Terminal Protein and their Corresponding Mobile Amino Acid Residues and IgA Reactivity.

Reactive Peptides from IgA epitope analysis	Corresponding amino acid residues	Corresponding accessible amino acid residues from mobility plot
2-3	8-28	18-25
9-13	57-98	70-76
23	155-168	147-165
26	176-199	-
29-30	197-317	-
32	219-231	216-225
37	253-266	252-259
41	281-294	273-286
44-45	302-329	315-328

* Data obtained based on Figure 3.16

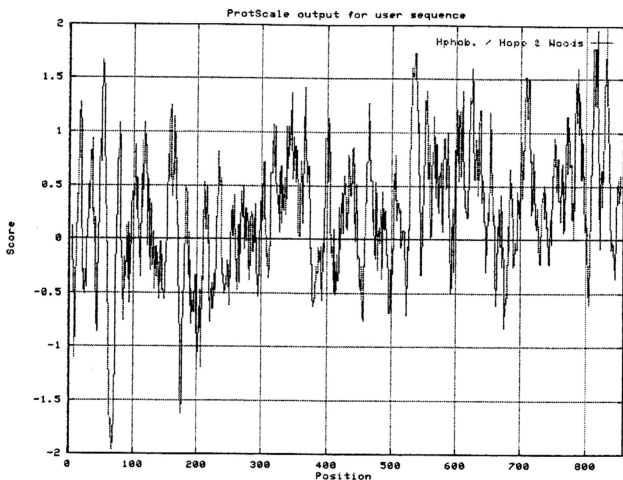


Figure 3.24 : Hydropathy plot for the 858 amino acid of the HHV6 p101 nucleocapsid protein. From this plot, amino acids from the most hydrophilic region at the carboxyl terminal were selected to be synthesized.

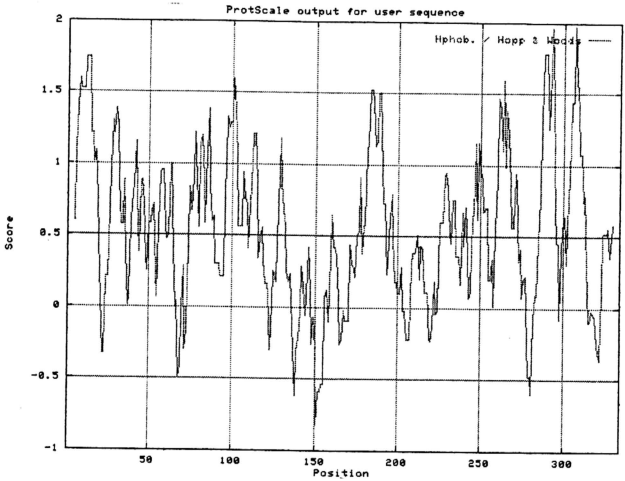


Figure 3.25 : Hydropathy plot for amino acid 524 - 858 (334 amino acid) of the p101 carboxyl terminal protein of HHV6.

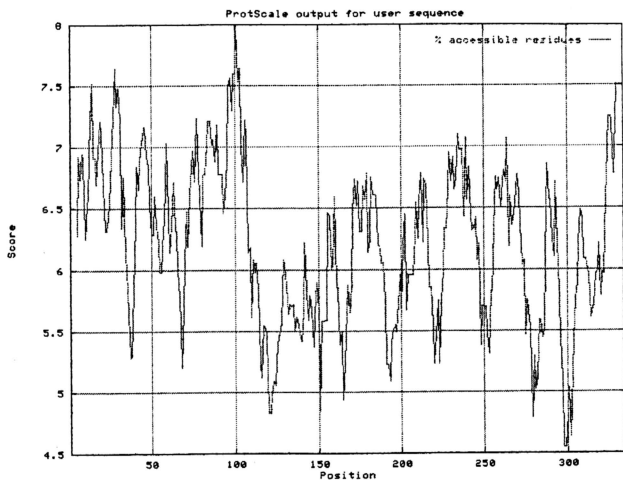


Figure 3.26 : Surface accessible region plot for the 334 amino acids of the p101 carboxyl terminal protein of HHV6.

```

0_seq1YU VSLIKDLRDK DGFRKQKKLD LLGSWTKEKN DKAIVHSREV TGDSDGDATE
1_seq1YU VSLIKDLRDK DGFRKQKKLD LLGSWTKEKN DKAIVHSREV TGDSDGDATE
2_seq1YU VFLIKDLRDK DGFRKQKQSD IPKSLTKERN DKAIMHSREV TGDSDGDATE
DSC_SEC CCHHHHHHCCC HHHHHHHHCCC HHHHHHHHCCC CCCEEEEEEE CCCCCCCCCC
PROB_H 2248865434 5679976744 5555655533 4443122221 111112221
PROB_E 2321100010 0000000111 2000010011 0115664445 3111001267
PROB_C 6541145666 5431134255 3555445566 6552124444 6888997622

0_seq1YU VTARDSPVLR KTKHANDIFA GLNKKYARDV SRGGKGNRSR LYSGGNAEKK
1_seq1YU VTARDSPVLR KTKHANDIFA GLNKKYARDV SRGGKGNRSR LYSGGNAEKK
2_seq1YU VGARNSPALR KIKQANDFFA GLNKKNDRDV LRGGKGNKSD LHSGGNAKKK
DSC_SEC ECCCCCHHHH HHHHHHHHHH HHHCCCHHHH HHCCCCCCCC CHHCCCCCCC
PROB_H 1122226999 9966666999 6654457999 9841111134 4752113344
PROB_E 7521100000 0000000000 0001000000 0100011231 1100001111
PROB_C 2467704111 1144441111 4455653111 1169980745 5258996655

0_seq1YU ETSGKFNVDK EMTQNEQEPL PNLMEAAARNA GEEQYVQAGL GQRVKNILAE
1_seq1YU ETSGKFNVDK EMTQNEQEPL PNLMEAAARNA GEEQYVQAGL GQRVKNILAE
2_seq1YU EMSGKFNDLK EMTRNGQEPS RSLMGDARNA GDEQYIQAGL GQRVNNLLSQ
DSC_SEC CCCCCCCCCC CHHCCCCCCC HHHHHHHHHH HHHHHHHHCCC CHHHHHHHHH
PROB_H 3411212234 4654333234 9999999976 5799997833 3569999998
PROB_E 1222343311 100011010 0000000000 0000011111 1000000001
PROB_C 4577555565 5456666866 1111111134 5311002166 6541111111

0_seq1YU FTNLISLGEK GIQDILHNQS GTELKLPTEN KLGRESEAN VERILEVSDP
1_seq1YU FTNLISLGEK GIQDILHNQS GTELKLPTEN KLGRESEAN VERILEVSDP
2_seq1YU FTNLISLGEK GIEDILQNR GTELKLATEN KSGRESEAN VEKILEVSNP
DSC_SEC CCHHHHHHCCC CCHHHHHHCCC CCCCCCCHH HHHHHHHHHH HHHHHHHHCCC
PROB_H 8877775444 4699978543 2231112255 6656777776 9999975213
PROB_E 1111110010 0000111001 0234442200 0000000000 0001010001
PROB_C 1122225656 6411021566 8645556655 4454333334 1110125896

0_seq1YU QNLFKNFKLQ NDLDVQSPFF RLPNADLSRD LDSVSFKDAL DVKLPGNGER
1_seq1YU QNLFKNFKLQ NDLDVQSPFF RLPNADLSRD LDSVSFKDAL DVKLPGNGER
2_seq1YU QDMFKNFRLQ NDLDVQSPFF RLPDADLSRE LDSASFKDAL DLKLPGNGER
DSC_SEC HHHHHHHHCCC CCCCCCCCCC CCCCCCHHH HHHHHHHHHH EEECCCCCHH
PROB_H 6799985331 1123322122 2123445577 9786566554 1101111359
PROB_E 0000012331 1001111111 1101000000 0011110012 6662000100
PROB_C 4311113448 8986677877 7886665533 1313434544 3347999651

0_seq1YU EIDLALQKVK AGERETSDFK VGQDETLPIT QLMKVETPEE KDDVIEKMVL
1_seq1YU EIDLALQKVK AGERETSDFK VGQDETLPIT QLMKVETPEE KDDVIEKMVL
2_seq1YU EIDLALQKVK VGETETSDLK VGQDESFPVA QLMKVETPEE KDDVIEQMVL
DSC_SEC HHHHHHHHHH CCCCCCEEE CCCCCCCHH HHHCCCCCCC CCHHHHHHHH
PROB_H 9999999975 4344444222 211222257 7763221121 2469999995
PROB_E 0000000011 0100011444 3101223321 113211000 0000000104
PROB_C 1111111124 6666655444 5897665532 2234678989 8641111001

0_seq1YU RIRQDGETDE ETVPGPGVAE SLGIAAKDKS VIAS
1_seq1YU RIRQDGETDE ETVPGPGVAE SLGIAAKDKS VIA:
2_seq1YU RIRQDGETDE NTVSGPGVAE SLDIEAKGES AIA:
DSC_SEC EEECCCCCCC CCCCCCCHH HHHCCCCCCC CCCC

```

Figure 3.27 : Secondary structure predictions for amino acids 1 to 334 of the p101 carboxyl terminal protein of HHV6 according to DSC programme by Protoscale. The secondary are in colour and the amino acids are in black print. [C = coils, E = sheet, H = helix]

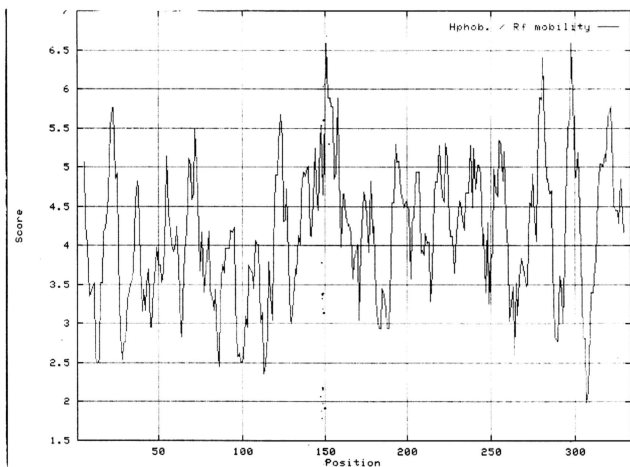


Figure 3.28 : Mobility plot for the 334 amino acids of the p101 carboxyl terminal protein of HHV6.

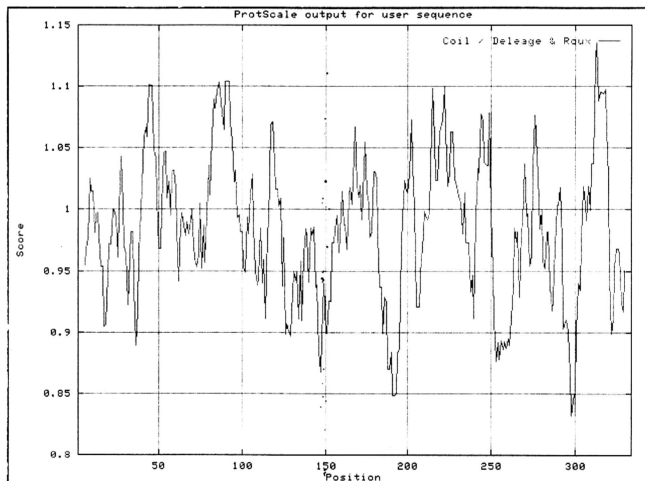


Figure 3.29 : Coil structured region plot for the 334 amino acids of the p101 carboxyl terminal protein of HHV6.